

基于平坦相干超连续谱的近红外光梳光谱技术

张静^{1,2*}, 蔡玉汝^{1,2**}, 黄勤清^{1,2}, 周文^{1,2}, 程林^{1,2}

¹南瑞集团有限公司(国网电力科学研究院), 江苏 南京 211006;

²国网电力科学研究院武汉南瑞有限责任公司, 湖北 武汉 430074

摘要 研究了相干度高且光谱平坦的近红外超连续谱(SC)光梳的产生以及超宽带光梳光谱的测量问题。利用掺铒光纤光梳脉冲抽运高非线性色散位移光纤, 获得光谱覆盖范围为 1250~1900 nm 的平坦 SC, 并通过理论模拟和实验验证了 SC 的高相干性。同时, 在该 SC 光梳源的基础上, 利用傅里叶变换光谱技术, 对包含 HF、¹²C₂H₂、¹²CO、H₂O 的混合气体样品进行超宽带高分辨分子光谱测量。实验得到的数据与 HITRAN2012 数据库模拟的结果一致, 误差小于 1.6%, 验证了基于平坦 SC 光梳光谱测量多组分气体的可行性。

关键词 非线性光学; 超连续谱; 相干特性; 光纤光学

中图分类号 O436

文献标志码 A

doi: 10.3788/CJL202148.0711003

1 引言

光学频率梳(OFC)即光梳是一种具有时频稳定性的相干光源^[1], 在频率域体现为一系列具有窄线宽特性且等间距分布的频率梳齿集合。光梳改变了传统分子光谱测量方式, 使同时对成百上千条分子谱线进行快速高分辨测量成为可能^[2]。光梳光谱技术^[3]已成为当今光谱技术领域的研究热点, 推动了光学相干层析^[4]、痕量分析^[5]以及光学遥感^[6]等领域的技术变革。但光梳谱宽受光源增益带宽的限制, 在超宽带光谱测量方面的应用仍不及传统傅里叶变换光谱技术, 限制了其在化学分析以及大气环境监测等领域的应用^[1-3]。

目前, 超连续谱(SC)产生技术是拓展光源光谱宽度的主要途径, 其基本原理是利用超短脉冲抽运非线性介质如光子晶体光纤或高非线性光纤(HNLF)^[7-9]引发自相位调制(SPM)、四波混频(FWM)以及受激拉曼散射(SRS)等非线性效应, 产生新的频谱成分, 最终实现超宽带光谱覆盖^[10]。但光纤中传输的光脉冲在色散作用下会出现脉冲宽度增宽、峰值功率下降的问题, 从而降低非线性效应, 制约了 SC 的产生。因此, 通常选用在抽运光波段

表现为反常色散特性的非线性光纤, 通过孤子效应维持高效的非线性展宽过程, 进而获得可覆盖一个甚至多个倍频层的 SC, 但会导致强非线性效应以及相位调制不稳定, 使 SC 光谱出现强烈的幅度振荡与抖动, 还会引入附加相位(频率)噪声, 出现明显的退相干现象, 这些问题严重限制了 SC 产生技术在光梳以及光谱测量中的应用。

近年来, 人们发现在抽运波长处近零色散的非线性光纤中存在的自相似效应与四波混频效应有助于平坦 SC 的形成^[11], 并逐渐将 SC 光梳应用于高精度光梳光谱分析等研究中。Millot 等^[12]利用色散补偿光纤(DCF)产生了光谱平坦的近红外光梳, 并基于双光梳干涉原理进行了高分辨气体分子光谱的测量。该研究强调了宽谱带平坦光梳源对精密分子光谱测量的重要性, 特别是在光谱背景拟合、谱线归一化、数据采集动态范围以及信噪比等方面具有积极作用。Nishizawa 等^[13]将掺铒光纤光梳与色散控制的 SC 产生技术相结合, 实现了光谱覆盖范围为 1.0~2.2 mm 的高相干度、高平坦度 SC 光梳源; 并将 SC 光梳与稳频窄线宽连续波(CW)激光器进行拍频探测, 利用拍频线宽表征 SC 的相位噪声特性, 在实验上验证了 SC 光梳的宽带相干性。

收稿日期: 2020-08-26; 修回日期: 2020-10-10; 录用日期: 2020-11-11

基金项目: 国网电力科学研究院有限公司(524625180044)

*E-mail: 275256470@qq.com; **E-mail: sxyccyr@163.com

目前,对基于超宽带平坦相干SC的光梳光谱研究较少,且SC的相干性与相位噪声特性仍需理论与实验研究的结合。针对上述问题,本文选用高非线性色散位移光纤(HNL-DSF),在光纤光梳脉冲的抽运下,产生了光谱范围为1250~1900 nm的平坦SC光梳源。通过数值求解非线性薛定谔方程(NLSE)模拟了SC的产生及其相干性与噪声分布特性,并利用稳频CW激光拍频探测光梳齿线宽的方式,验证了SC光梳的相干性。利用该光源,实现了对混合气体样品的高分辨近红外光谱测量,实验结果与基于HITRAN2012数据库模拟的结果一致,验证了超宽带SC光梳光谱测量多组分气体的可行性。

2 实验装置与结果分析

2.1 超连续谱的产生

实验装置如图1所示,其中,ISO为光隔离器,Gas为气体样品池,FTS为傅里叶变换光谱仪。采用一台非线性偏振旋转(NPR)锁模的光纤光梳作为种子源^[14-15],其中心波长为1560 nm,全光谱宽为100 nm。光梳源的输出脉冲宽度为650 fs,重复频率为54.5 MHz,平均功率小于10 mW。光梳的重复频率(f_r)以及载波包络相位零频(f_0)锁定后的精度分别为1 mHz和10 mHz。为了提高光功率,实现非线性光谱展宽,种子光经过长为2 m的单模保偏光纤(PMF)后进入一台双向泵浦的掺铒光纤放大器(EDFA),放大的光功率为100 mW。EDFA中的增益光纤(Er80-4/125-HD, Liekki)具有正色散系数,该增益光纤通过色散补偿作用,可以将脉冲宽度压缩为100 fs。为了获得高相干度的平坦SC,放大脉冲通过光纤耦合器注入一段HNL-DSF(Yofc)。该光纤在零色散波长1550 nm处的色散斜率小于0.03 ps/(nm²·km),衰减系数小于1.5 dB/km。通过光谱分析仪(AQ6375B, Yokogawa,分辨率为0.2 nm)对HNL-DSF输出的SC进行测量,其光谱范围为1250~1900 nm,覆盖了HF、CO、C₂H₂、CH₄等分子振动的倍频(overtone)与组合振动(combination tone)吸收谱峰群;且在1400 nm与1800 nm处出现了两个平滑的光谱区间,这有利于光谱轮廓的拟合与归一化处

理,从而提升系统对复杂且密集分布分子谱线的测量精度。

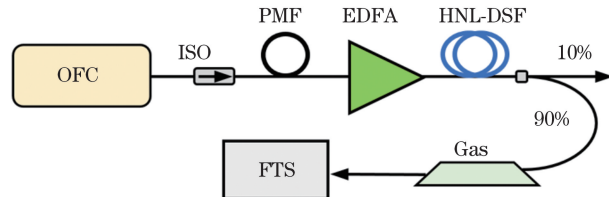


图1 实验装置图

Fig. 1 Diagram of the experimental setup

图2为非线性光纤展宽前后的光谱,同时,对比了正色散HNLF的光谱展宽结果。可以发现,在相同抽运光条件下,HNLF输出的SC谱宽更宽,约为HNL-DSF的1.5倍,但其光谱信噪比较低,且平坦性差,难以应用于多种类分子光谱的同时测量。实际中,反常色散区的光谱展宽主要依赖于孤子压缩效应,该效应和调制不稳定性都会导致平坦度劣化^[16-17];对于HNL-DSF,抽运波长处于近零色散的正常色散区间,产生的光谱更平坦。因此,非线性光纤的色散控制是提高SC谱平滑度的关键^[18-20]。

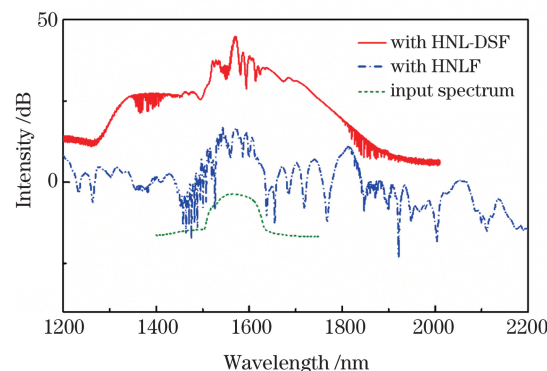


图2 非线性光纤展宽前后的光谱

Fig. 2 Spectra before and after nonlinear fiber broadening

2.2 数值模拟

SC产生过程中存在的强非线性效应以及高阶色散效应可能会在光脉冲中引入附加相位噪声以及强度涨落,影响光梳传输的时频相干特性,并限制其对分子谱线测量的信噪比与精度。为了研究SC的相干度与噪声特性,对HNL-DSF中光谱的时频特性进行了数值模拟。用分步傅里叶算法求解NLSE^[16],NLSE可表示为

$$\frac{\partial A(z, t)}{\partial z} = -\frac{\alpha}{2} A + \sum_{n \geq 1} \beta_n \frac{i^{n+1}}{n!} \frac{\partial^n}{\partial \tau^n} A(z, t) + i\gamma \left(1 + i\tau_{\text{shock}} \frac{\partial}{\partial t}\right) \left[A(z, t) \int_{-\infty}^{\infty} R(\tau) |A(z, t - \tau)|^2 d\tau \right], \quad (1)$$

式中, $A(z, t)$ 为脉冲光场的慢变包络, A 为光场的幅度, γ 为光纤的非线性系数, β 为高阶色散系数, z 为光的传播距离, t 为时间, α 为损耗系数, n 为色散阶数, τ 为响应时间, $R(\tau) = (1 - f_R) \delta(\tau) + f_R h_R(\tau)$, f_R 为拉曼常数, $h_R(\tau)$ 为时域拉曼响应函数^[16], $\delta(\tau)$ 为狄拉克函数, τ_{shock} 为光纤传输中的自抖动效应, 可表示为

$$\tau_{\text{shock}} \approx \frac{1}{\omega_0} - \left[\frac{1}{n_{\text{eff}}} \frac{dn_{\text{eff}}(\omega)}{d\omega} \right]_{\omega_0} - \left[\frac{1}{A_{\text{eff}}} \frac{dA_{\text{eff}}(\omega)}{d\omega} \right]_{\omega_0}, \quad (2)$$

式中, ω_0 为光场中心频率, n_{eff} 和 A_{eff} 分别为非线性光纤的有效折射率和有效截面。求解时 $\alpha=0$, $f_R=0.2$, $\gamma=11.9 \text{ W}^{-1} \cdot \text{km}^{-1}$, $\beta_2=0.001294 \text{ ps}^2/\text{m}$, $\beta_3=4.827 \times 10^{-5} \text{ ps}^2/\text{m}$, $n_{\text{eff}}=3.2 \times 10^{-20} \text{ m}^2/\text{W}$, $A_{\text{eff}}=4.5 \mu\text{m}^2$, HNL-DSF 的长度为 3.3 m。NLSE 的计算结果如图 3(a) 所示。可以发现, 在 1400 nm 与 1800 nm 波长处出现两个平滑的光谱区间, 这与实验结果一致。但实验得到的光谱数据在 1400 nm 处强度较低, 且在 1800~2200 nm 区间强度下滑, 原因是计算中未考虑大气中水分子在 1350~1400 nm 与 1800~1900 nm 附近的强吸收效应以及光学元件与探测器响应曲线的影响。

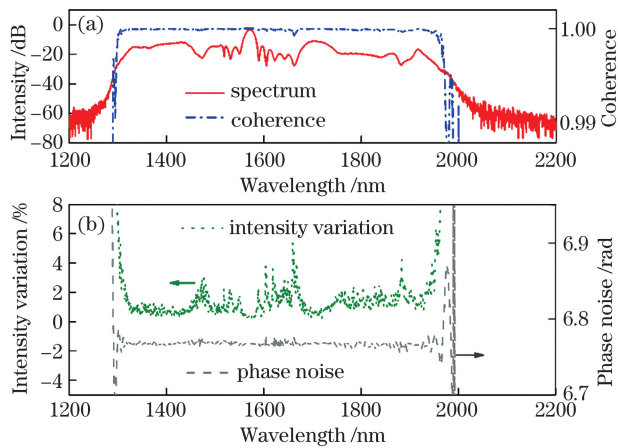


图 3 SC 数值模拟的结果。(a)理论模拟的 SC 强度及相干度;(b)SC 的相对强度与相位噪声

Fig. 3 Results of SC the numerical simulation. (a) SC intensity and coherence of the theoretical simulation; (b) relative intensity of the SC and phase noise

SC 光谱的一阶相干性 $g(\omega)$ 可表示为^[17]

$$g(\omega) = \frac{|\langle \tilde{A}_i(\omega) \tilde{A}_j^*(\omega) \rangle_{i \neq j}|}{\sqrt{\langle |\tilde{A}_i(\omega)|^2 \rangle \langle |\tilde{A}_j(\omega)|^2 \rangle}}, \quad (3)$$

式中, $\tilde{A}_i(\omega)$ 和 $\tilde{A}_j(\omega)$ 分别为第 i 和 j 个光梳梳齿的光场幅值函数, 上标 * 表示该函数的共轭。模拟

中引入了随机量子噪声 (Quantum noise), 可根据(3)式计算 SC 光谱范围内的光梳梳齿相干性。从图 3(a) 可以发现, 光梳在 SC 产生过程中保持了较好的相干性, 即 $g(\omega)$ 约为 1, 且在宽谱范围内具有一致性。当 $g(\omega)=1$ 时, 认为梳齿之间具有完全相干性。

统计分析了模拟的 20 组 SC 强度与相位的标准方差, 得到的相对强度抖动以及相位噪声分布情况如图 3(b) 所示。可以发现, 在光谱覆盖范围内光强度的相对抖动量约为 2%, 在 1400 nm 平坦光谱区间内的强度抖量约为 1%。同时, SC 光梳的相位在非线性效应与色散作用下出现了整体偏移 (偏移量为 6.77 rad), 在整个光谱范围内的相位噪声小于 10 mrad。这表明 HNL-DSF 产生的 SC 稳定性好、相位噪声小且对光梳的时频相干性影响较小。由于光梳展宽过程受到自相位调制与光纤中拉曼效应的影响, 其在 1480 nm 和 1700 nm 波长附近的光谱能量较小, 且强度调制明显, 对应梳齿的强度抖动与相位噪声相对较大。

2.3 拍频探测实验

通过测量光梳梳齿线宽的方式检测 SC 的时频相干性, 实验对比了光梳在 SC 产生前后的梳齿线宽。采用两台中心波长分别为 1535.4 nm 与 1550.5 nm 的超窄线宽 CW 激光器 (Koheras BASIK E15 系列, NKT Photonics; -3 dB 线宽小于 1 kHz), 分别与光梳源及 SC 进行光外差拍频探测^[12], 以验证光谱展宽前后的梳齿相干性。测量中, 待测光先后与窄线宽 CW 激光由一个分光比为 50:50 的光纤耦合器合束, 并在平衡探测器 (PDB480C-AC, Thorlabs; 带宽为 1.6 GHz) 上进行拍频探测。探测信号由频谱分析仪 (NSA1036-TG, Owon; 频谱宽度为 3.6 GHz) 记录。图 4(a) 和图 4(b) 分别为 1535.4 nm CW 激光与原始光梳、SC 的拍频信号 (分辨率带宽 RBW: 3 kHz), 其中, b 表示拍频信号, 下标表示拍频的波长, 1 和 2 分别表示非线性光谱展宽前后的信号。10 次测量取平均值, 得到光谱展宽前后拍频信号的 -3 dB 线宽处分别为 (2.7 ± 1.0) kHz 和 (2.6 ± 1.0) kHz。受频谱仪分辨率的限制, 实验未发现明显的拍频信号线宽加宽现象, 这表明在光谱展宽过程中由 HNL-DSF 引入的相位噪声较小, 在一定程度上, SC 保持了种子光梳的相干性。图 4(c) 和图 4(d) 为在 1550.5 nm 处的测量结果, 选择在 1550.5 nm 处进行测量的原因是实验使用的窄线宽激光器波长为 1550.5 nm。

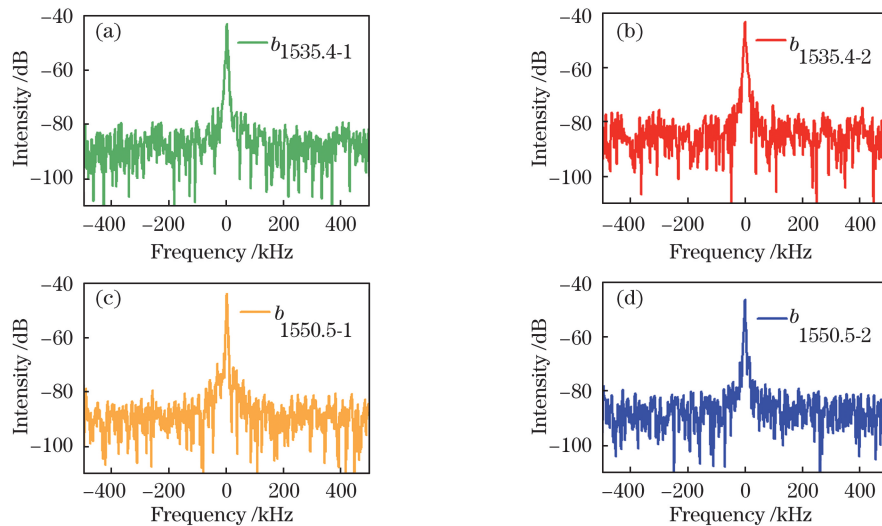


图4 非线性光谱的信号。(a)~(b)1535.4 nm 处激光展宽前后的信号;(c)~(d)1550.5 nm 处激光展宽前后的信号

Fig. 4 Signal of the non-linear spectrum. (a)–(b) Signals before and after laser broadening at 1535.4 nm; (c)–(d) signals before and after laser broadening at 1550.5 nm

实验测得的光谱展宽前后拍频信号线宽基本一致,分别为 (2.0 ± 1.0) kHz 和 (1.8 ± 1.0) kHz。

综上所述,光梳梳齿在 1550 nm 波长附近的相干度接近于 1,这表明光梳的光谱展宽过程对梳齿线宽的影响较小。此外,受窄线宽 CW 激光源的限制,实验仅在两个特定波长处对 SC 的相干性进行了验证,但在一定程度上说明了 SC 的宽带相干特性。实际上,相干光源是实现高分辨分子光谱测量的关键^[3],光源(梳齿)的线宽会限制光谱测量的分辨率与精度^[12]。因此,高相干度或窄梳齿线宽 SC 光梳的产生有利于在宽谱范围内实现高精度分子谱线测量。

2.4 混合气体的光谱测量

为了验证 HNL-DSF 中产生的高相干度平坦 SC 在光梳光谱测量中的可靠性,利用该光源对包含 HF、¹²C₂H₂、¹²CO 的混合气体样品进行了高分辨光谱测量。实验中,气体样品为两个光纤耦合的标准气体样品池,长度分别为 2.7 cm 与 5.5 cm,分别充有 HF 气体(6666.1 Pa)以及¹²CO(19998.3 Pa)与¹²C₂H₂(6666.1 Pa)气体。采用自行搭建的高分辨傅里叶变换光谱仪测量光谱,其谱分辨率率为 0.1 cm⁻¹(3 GHz)。受光学元件与探测器的限制,光谱仪的最优响应波段为 1200~1500 nm。测量结果如图 5 所示,可以发现,该实验装置能对包括 HF(1250~1330 nm)、¹²C₂H₂(1510~1540 nm)、¹²CO(1578~1585 nm)以及光路中的水分子 H₂O(1350~1480 nm)在内的多种气体分子光谱进行同

时测量,测量时间仅为 0.1 s。

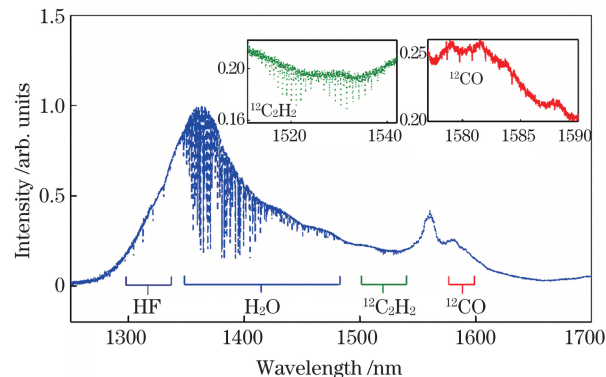


图5 宽带近红外单光梳分子的吸收光谱

Fig. 5 Absorption spectrum of the broadband near-infrared single comb molecule

为了验证光谱测量的准确性,将实验结果与 HITRAN2012 数据库模拟的结果进行对比。得益于 SC 的平坦性,简单的多项式拟合就能达到良好的光谱归一化效果,归一化的 HF 吸收谱如图 6 所示。光谱数据模拟中,利用 Viogt 线型^[21],结合 HITRAN2012 数据库的谱线信息以及气体样品的测量条件(温度为 297 K,气压为 6666.1 Pa,谱线分辨率为 0.1 cm⁻¹)计算 HF 的吸收峰。可以发现,实验与模拟结果相吻合,两者偏差的均方差仅为 1.6%,主要受限于 SC 自身的强度噪声。由于 HF 是电力设备故障检测中的目标气体之一^[22],对多个 HF 指纹峰的准确测量,有利于提高气体检测准确度,因此具有重要应用价值。

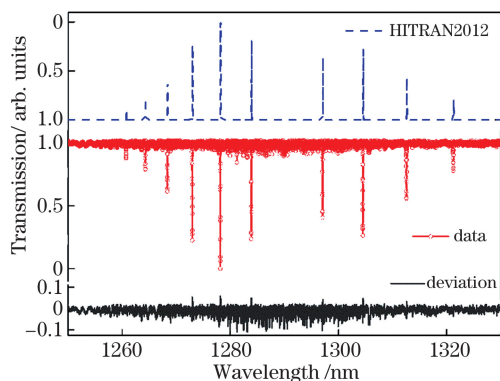


图 6 光谱数据与 HITRAN2012 数据库谱线的对比
Fig. 6 Comparison of spectral data and HITRAN2012 database spectral lines

3 结 论

利用掺铒光纤光梳脉冲抽运 HNL-DSF, 产生了光谱覆盖范围为 1250~1900 nm 的超宽带平坦 SC。数值模拟与实验结果表明, 该 SC 保持了光梳源的相干性。此外, 实验结合傅里叶变换光谱技术, 实现了超宽带近红外分子光谱的高分辨测量。实验数据与 HITRAN2012 数据库中的模拟结果一致, 这表明该超宽带相干 SC 光梳可为多组分气体同时且高速、高分辨光谱检测提供可靠的光源。

参 考 文 献

- [1] Udem T, Holzwarth R, Hänsch T W. Optical frequency metrology[J]. Nature, 2002, 416(6877): 233-237.
- [2] Weichman M L, Changala P B, Ye J, et al. Broadband molecular spectroscopy with optical frequency combs [J]. Journal of Molecular Spectroscopy, 2019, 355: 66-78.
- [3] Coddington I, Newbury N, Swann W. Dual-comb spectroscopy[J]. Optica, 2016, 3(4): 414-426.
- [4] Jung E J, Lee J H, Rho B S, et al. Spectrally sampled OCT imaging based on 1.7- μm continuous-wave supercontinuum source[J]. IEEE Journal of Selected Topics in Quantum Electronics, 2012, 18(3): 1200-1208.
- [5] Schroeder P J, Wright R J, Coburn S, et al. Dual frequency comb laser absorption spectroscopy in a 16 MW gas turbine exhaust[J]. Proceedings of the Combustion Institute, 2017, 36(3): 4565-4573.
- [6] Rieker G B, Giorgetta F R, Swann W C, et al. Frequency-comb-based remote sensing of greenhouse gases over kilometer air paths[J]. Optica, 2014, 1(5): 290-298.
- [7] Klimczak M, Siwicki B, Skibinski P, et al. Mid-infrared supercontinuum generation in soft-glass suspended core photonic crystal fiber[J]. Optical and Quantum Electronics, 2014, 46(4): 563-571.
- [8] Belli F, Abdolvand A, Chang W, et al. Vacuum-ultraviolet to infrared supercontinuum in hydrogen-filled photonic crystal fiber[J]. Optica, 2015, 2(4): 292-300.
- [9] Zhan Y, Wang L. Coherence properties of supercontinuum based on photonic crystal fiber[J]. Acta Optica Sinica, 2013, 33(F06): s119001. 詹仪, 王丽. 光子晶体光纤产生超连续谱相干特性的研究[J]. 光学学报, 2013, 33(F06): s119001.
- [10] Ahmed J, Siyal M Y, Adeel F, et al. Supercontinuum generation by nonlinear optics[M]// Optical Signal Processing by Silicon Photonics. SpringerBriefs in Materials. Singapore: Springer, 2013: 69-79.
- [11] Liang T, Feng X M. Research progress toward flat supercontinuum generation in fibers[J]. Laser & Optoelectronics Progress, 2016, 53(6): 060002. 梁田, 冯小妹. 利用光纤产生平坦超连续谱的研究进展[J]. 激光与光电子学进展, 2016, 53(6): 060002.
- [12] Millot G, Pitois S, Yan M, et al. Frequency-agile dual-comb spectroscopy[J]. Nature Photonics, 2016, 10(1): 27-30.
- [13] Nishizawa N, Niinomi T, Nomura Y, et al. Octave spanning coherent supercontinuum comb generation based on Er-doped fiber lasers and their characterization[J]. IEEE Journal of Selected Topics in Quantum Electronics, 2018, 24(3): 1-9.
- [14] Shen X L, Yan M, Hao Q, et al. Adaptive dual-comb spectroscopy with 1200-h continuous operation stability[J]. IEEE Photonics Journal, 2018, 10(5): 1503309.
- [15] Yan M, Hao Q, Shen X L, et al. Experimental study on polarization evolution locking in a stretched-pulse fiber laser[J]. Optics Express, 2018, 26(13): 16086-16092.
- [16] Ruehl A, Martin M J, Cossel K C, et al. Ultrabroadband coherent supercontinuum frequency comb[J]. Physical Review A, 2011, 84: 011806.
- [17] Blow K J, Wood D. Theoretical description of transient stimulated Raman scattering in optical fibers [J]. IEEE Journal of Quantum Electronics, 1989, 25(12): 2665-2673.
- [18] Dai S X, Wang M, Wang Y Y, et al. Review of mid-infrared supercontinuum spectrum generation based on chalcogenide glass fibers [J]. Laser & Optoelectronics Progress, 2020, 57(7): 071603. 戴世勋, 王敏, 王莹莹, 等. 基于硫系玻璃光纤的中红外超连续谱产生研究进展[J]. 激光与光电子学进展, 2020, 57(7): 071603.

- 展, 2020, 57(7): 071603.
- [19] Zhang T T, Shi W H. Numerical research on ultraviolet supercontinuum generation in photonic crystal fiber[J]. Chinese Journal of Lasers, 2020, 47(3): 0301012.
张甜甜, 施伟华. 光子晶体光纤产生紫外超连续谱的数值研究[J]. 中国激光, 2020, 47(3): 0301012.
- [20] Li Z X, Gong C, Hua L Q, et al. Supercontinuum generation in calcium fluoride crystals using high-intensity femtosecond laser[J]. Chinese Journal of Lasers, 2019, 46(5): 0508021.
李子熙, 龚成, 华林强, 等. 强飞秒激光在氟化钙晶
- 体中产生的超连续谱[J]. 中国激光, 2019, 46(5): 0508021.
- [21] Valenti J A, Piskunov N. Spectroscopy made easy: a new tool for fitting observations with synthetic spectra[J]. Astronomy and Astrophysics Supplement Series, 1996, 118(3): 595-603.
- [22] Zhao K, Jiang M, Li P, et al. Research on on-line infrared spectrometer measurement for SF₆ decomposition gases[J]. Navigation and Control, 2017, 16(3): 85-90.
赵坤, 姜萌, 李磐, 等. SF₆分解气的近红外在线检测技术研究[J]. 导航与控制, 2017, 16(3): 85-90.

Near-Infrared Comb Spectroscopy Technology Based on Flat Coherent Supercontinuum

Zhang Jing^{1,2*}, Cai Yuru^{1,2**}, Huang Qinqing^{1,2}, Zhou Wen^{1,2}, Cheng Lin^{1,2}

¹ NARI Group Corporation (State Grid Electric Power Research Institute), Nanjing, Jiangsu 211006, China;

² Wuhan NARI Co Ltd., State Grid Electric Power Research Institute, Wuhan, Hubei 430074, China

Abstract

Objective Optical frequency comb (OFC) is a coherent light source with excellent time-frequency stability. In frequency domain, an OFC is a set of frequency comb teeth with narrow linewidth and equidistant distribution. Because of this characteristic, the OFC has revolutionized the approach to molecular spectroscopy, making it possible to simultaneously and rapidly measure hundreds of molecular spectral lines with high resolution. The OFC spectroscopy technology has become a hot spot in the field of spectral technology, and has promoted the technological changes in the fields of optical coherence tomography, trace analysis and optical remote sensing. However, due to the limitation of the light source gain bandwidth, the comb spectrum is still unable to compare with the traditional Fourier transform spectroscopy technology in ultra-wideband spectrum measurement, which limits its applications in, such as chemical analysis and atmospheric environment monitoring. At present, supercontinuum (SC) generation technology is the main way to expand the spectral width of light sources. However, the strong nonlinear effect and phase modulation instability inside nonlinear fibers will not only cause strong amplitude oscillation and jitter of SC spectrum, but also introduce additional phase (frequency) noise, resulting in obvious decoherence. These problems seriously limit the application of SC generation technology in comb and spectrum measurement. Here, the generation of near infrared SC comb with high coherence and flat spectrum is investigated. The coherence is confirmed by beat note measurements and nonlinear Schrödinger equation (NLSE) based numerical simulation. The source could be useful for broadband gas sensing in monitoring of electrical installations.

Methods First, an erbium-doped fiber comb is harnessed for producing a flat SC with spectral coverage of 1250–1900 nm in a high nonlinear dispersion shifted fiber(HNL-DSF). A home-made nonlinear-polarization-rotation (NPR) mode-locked fiber laser comb delivered a train of 650 fs pulses at a repetition rate of 54.5 MHz with 10 mW of average output power (**Fig. 1**). The output pulses are temporally chirped with a 2 m-long single mode fiber (SMF) and then amplified by a bidirectional pumped erbium-doped fiber amplifier (EDFA) with an output power up to ~100 mW. The EDFA also behaves as a fiber compressor, producing pulses of sub-100 fs which is directly injected into a 200 m-long HNL-DSF (Yofc) for SC generation with a flat spectral profile. The HNL-DSF had a zero dispersion wavelength around 1550 nm (dispersion slope of 0.03 ps/(nm² · km); loss coefficient <1.5 dB/km; nonlinear coefficient >10 W⁻¹ · km⁻¹). Second, beat note measurements between the original spectrum (and SC) and two stable continuous-wave (CW) lasers at 1550.5 nm or 1535.4 nm are performed for confirming the coherence of the SC. For investigating the coherence beyond the CW laser wavelengths, numerical simulation is performed, revealing pulse propagation inside the fiber, by solving NLSE using split step Fourier method. Wide-band first-order spectral

coherence is confirmed. Finally, the SC is launched for spectral measurements of a mixed gas sample, containing HF (6666.1 Pa), ^{12}CO (19998.3 Pa), $^{12}\text{C}_2\text{H}_2$ (6666.1 Pa), and the natural water vapor in the laboratory. The measurements are carried out with a home-made Fourier-transform spectrometer at a spectral resolution of 0.1 cm^{-1} . The temperature is 297 K.

Results and Discussions In the experiment, a broadband SC comb, spectrally spanning from 1250–1900 nm (**Fig. 2**) with good flatness around 1400 nm and 1800 nm, is achieved in a piece of DSF. The high coherence of SC is verified by theoretical simulation and experimental measurements. Simulation results show that the SC comb had a high coherence, $g(\omega) \sim 1$, and low phase noise (< 10 mrad) over a wide spectral range (**Fig. 3**). Experimentally, the beat notes between the 1550.5 nm/1535.4 nm laser and the comb and SC show linewidths at -3 dB of $(2.7 \pm 1.0)\text{ kHz}/(2.0 \pm 1.0)\text{ kHz}$ and $(2.6 \pm 1.0)\text{ kHz}/(1.8 \pm 1.0)\text{ kHz}$, respectively (**Fig. 4**). No obvious linewidth broadening is found, indicating the coherence remain unchanged in the nonlinear spectral broadening process. The absorption peak of water vapor in the near infrared region is measured around 1365 nm (**Fig. 5**). Meanwhile, the transition lines for HF (around 1300 nm), ^{12}CO (1580 nm), $^{12}\text{C}_2\text{H}_2$ (1560 nm) are measured simultaneously. For spectroscopic validation, the results of HF are compared with the simulation based on the parameters given by the HITRAN2012 database. The experimental results are consistent with the simulation results (deviation less than 1.6%, as shown in **Fig. 6**), indicating that the SC comb could be an excellent light source for multi-gas sensing as required by monitoring of electrical power equipment.

Conclusions In conclusion, ultra-broadband near-infrared SC generation is performed using a dispersion shifted high nonlinear fiber, pumped by $1.55\text{ }\mu\text{m}$ comb pulses. The excellent flatness and coherence of SC are investigated by numerical simulation and experimental beat-note measurements. As a result, high spectral coherence and low phase noise (< 10 mrad) are demonstrated for a wide spectral coverage. Particularly, the beat note linewidths between the initial comb and SC with two CW lasers confirm that the phase noise induced by the DSF, to a certain extent, is negligible, comparing to the comb line spacing (54.5 MHz). Furthermore, based on the SC comb source, Fourier transformed frequency comb spectroscopy is carried out for measuring ultra-broadband and high-resolution molecular spectra of mixed gases (HF, $^{12}\text{C}_2\text{H}_2$, ^{12}CO , H₂O). The experiment data are consistent with that simulated in HITRAN2012 database with standard deviation of less than 1.6%. We believe that flat SC based frequency comb spectroscopy will provide a promising approach for multi-gas sensing with high precision and high resolution.

Key words nonlinear optics; supercontinuum; coherence properties; fiber optics

OCIS codes 190.4370; 030.1670; 060.2310